Journal of Food Health and Bioenvironmental Science
Journal homepage : http://jfhb.dusit.ac.th/

Local Production and Characterization of Biochar from Bamboo Waste and the Removal of Natural Organic Matter from Nakhon Nayok River, Thailand

Dusit Angthararuk[a, b]* Sasamol Phasuk[a] & Pannraphat Takolpuckdee[a]

[a] *Faculty of Science and Technology, Valaya Alongkorn Rajabhat University under the Royal Patronage, Pathum Thani, 13180 Thailand*
[b] *Faculty of Science and Technology, Suan Dusit University, Bangkok, 10300 Thailand*

Article info

Article history:
Received : 22 January 2022
Revised : 5 April 2022
Accepted : 11 April 2022

Keywords:
Bamboo, Biochar, Characterization, NOM

Abstract

The objective of this research was to produce a biochar from bamboo handicraft waste via pyrolysis process using a modified 200 L steel drum kiln. The temperature outside the kiln-producing biochar appeared around 500-600°C, closely related to the temperature of slow pyrolysis. The physical and chemical properties of bamboo biochar (BB) were characterized by using proximate and ultimate analysis, Brunauer-Emmett-Teller surface area techniques, elemental analysis, scanning electron microscopy coupled with an energy dispersive spectroscopy, Fourier transform infrared spectroscopy, Raman spectroscopy and X-ray diffraction techniques. It was found that 28.76 ± 2.22% of BB yield with 77.07 ± 1.92 % fixed carbon. As the morphology properties, its surface area and total pore were 247.5 ± 7.1 $m^2 g^{-1}$ and 0.16 ± 0.02 $cm^3 g^{-1}$, respectively. Batch test for removal of natural organic matter (NOM) in Nakhon Nayok River, by adsorbed on BB was studied. The results showed that the percentage reduction of dissolve organic matter (DOC) and absorbance at 254 nm at equilibrium were 71.33 ± 1.46 and 76.51 ± 2.01, respectively, while the adsorption capacity was 4.75 $mg.g^{-1}$ DOC. Pseudo-second order kinetic model was best suited for describing the adsorption of DOC onto BB. This suggests that interaction of NOM on BB were explored in terms of multicomponent adsorption, which the heterogeneous distribution of the adsorptive sites at biochar surfaces. It was found that biochar is suitable for the adsorption of NOM from surface water and is a low-cost effective adsorbent in the treatment of wastewater. Biochar can be applied for a variety of purposes for example: as biofuels, adsorbents and as soil amendments. In addition, the biochar kiln is small and easy to create, creates no smoke, inexpensive, easy to use, does not take much time to produce and has an eco-friendly processing.

* Corresponding Author
e-mail: dusit_ang@dusit.ac.th

Introduction

High levels of natural organic matter (NOM) in surface water is a major concern for utilization of water. The presence of NOM molecules affects the color of water making the water appear yellow or brown (Ghernaout et al., 2014). NOM is an intricate mixture of organic compounds from decomposition of microbial, plants and animal waste. NOM can be a source for the formation of carcinogens such as trihalomethanes (THMs) and haloacetic acids (HAAs) that water is disinfected with chlorine. The elimination of NOM is essential by use of several physicochemical and biological methods, including, chemical precipitation, adsorption, filtration, reverse osmosis and coagulation. (Yehia & Said, 2021; Guillossou et al., 2020). However, these technologies encounter several disadvantages such as the removal efficiency of low-concentration pollutants are incomplete resulting in toxic products, high energy, chemicals and maintenance consumption (He et al., 2017). Biochar adsorption is an interesting choice, eco-friendly and low-cost material that adsorbed many pollutants from contaminated water (Srivatsav et al., 2020). Biochar is a carbon-rich solid material produced from decomposed organic matter, agricultural residue, wood waste, municipal waste and animal manures, by heating biomass precursors in an oxygen-limited environment (El-Hassanin et al., 2020; Wang et al., 2020; Yazdani et al., 2019). It has been reported to be able to ameliorate soil fertility by carbon sequestration, increasing water and nutrient retention (Dokmaingam et al., 2020; Song et al., 2019; Kätterer et al., 2019), furthermore, to reduce greenhouse gas emissions into the atmosphere (Al-Ghussain, 2019; Zhang et al., 2017). Moreover, biochar can remove various contaminants, including pathogenic organisms, organic contaminants such as dyes (Nguyen et al., 2021) and inorganics such as heavy metals (Shaheen et al., 2019).

Bamboo is a local resource that is valuable to the way of life of Thai people from the past to the present. The reason bamboo is valuable to Thai life is due to it being a fast-growing plant and multipurpose species are used from its rhizome/roots, clumps, shoots, leaves, leaf sheath, branch and culm. The study on bamboo growing in Thailand found that the commercial bamboo cultivation areas are scattered throughout the country, amounting to 91,746 rai. (approx.146.79 km^2) (Land Development Department, 2020). The Thai Wiang Community, Mueang District, Nakhon Nayok Province, Thailand (Fig. 1) has used bamboo in occupations such as handicraft, tree crutches and baked sticky rice in bamboo. The bamboo residue becomes community waste and is burnt in open fields. The burning of the bamboo waste contributes to global warming and increases the level of airborne particles (Lohan et al., 2018). Greenhouse gases (GHG) emissions caused by the burning of agricultural crops in Mae Chaem Basin, Chiang Mai Province, Thailand, was reported by Arunrat et al. (2018) and found average value emissions of CO_2, CO, CH_4, NO_x, SO_x $PM_{2.5}$ and PM_{10} were 9879.3, 253.0, 17.6, 11.7, 1.3, 29.3 and 39.1 kg ha^{-1} $year^{-1}$, respectively. This is serious air pollution that negatively affects the environment and human health.The weakness of conventional charcoal production for example, from earth kiln, pit kiln, brick kiln and horizontal 200 liter kiln, creates low quality of biochar due to the large

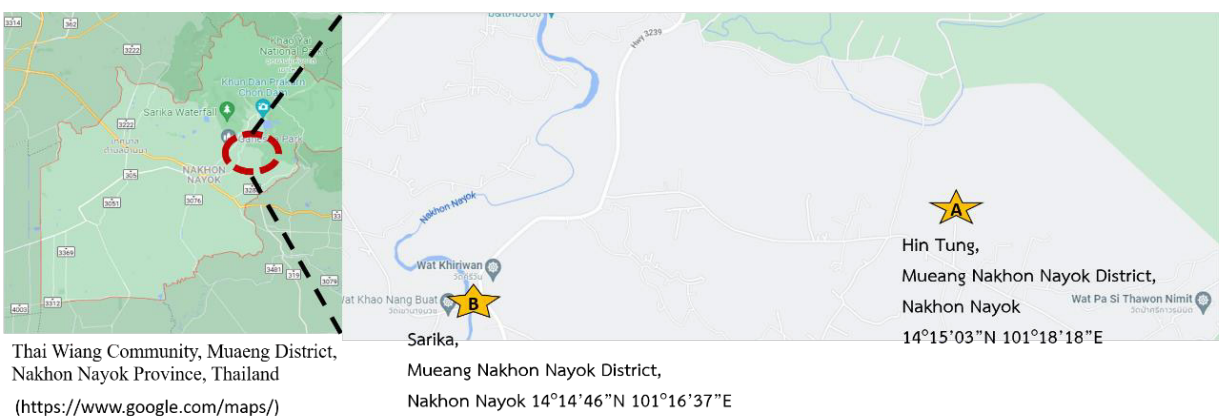

Fig. 1 Map of the Thai Wiang Community, Mueang District, Nakhon Nayok Province, Thailand; the place of (A) biochar production, (B) collected surface water from Nakhon Nayok River, by Google Earth™ mapping

amount of air entering the kiln during the burning process, long time operation of 1-3 days, smoke and inconvenient to use and move. The development of biochar kiln to produce quality biochar is interesting.

The objective of this research was to study the production of biochar from bamboo handicraft waste by local drum kiln via pyrolysis process and investigation of their properties and its application for removal of natural organic matter in Nakhon Nayok River, Thailand.

Materials and methods

1. Bamboo biomass

The bamboo handicraft waste used as feedstock for biochar production, were collected from the local area at Hin Tung, Mueang Nakhon Nayok District, Nakhon Nayok Province (14°15'03"N 101°18'18"E) showed in Fig.1 A. The dirt, sand and unwanted material from the surface of bamboo waste sample were removed and then dried in the open air for a week.

2. Biochar Production

Bamboo biochar (BB) was produced using a portable steel drum kiln made with available local resources allowing for low-cost production and easy to operate for local farmers. The steel drum kiln followed the design of O'Toole (2013) and was modified by added air vents at the bottom and upper zone as well as using 100 L of steel drum as flue for increasing air flow. In reference to Fig. 2, approximately 18 kg of bamboo materials (<10% moisture content) were filled in a small container (A) measuring 0.66 m in height and 0.37 m diameter then the lid was closed tightly to prevent oxygen entering during the pyrolysis process. The small container (A) was then placed upside down inside a larger container (B) (0.88 m height and 0.59 m diameter). The volume between the containers was filled with 20 kg of other bamboo waste, which was burnt for heating the inner container. The steel drum (C) was taken to cover the top to increase the air flow in the combustion. The combustion temperature surrounding 3 positions in each of 3 zones of the outer chamber were measured by non-contact handheld infrared thermometer (MESTEK IR01D). The biochar yield was calculated as follows: production yield (wt%) = (W_{BB}/W_{bamboo}) x 100, where W_{BB} was the weight of BB (kg) and W_{bamboo} was the weight of the bamboo biomass feedstock (kg) loaded into the kiln, both on a basis of dry weight. After the outer container wood waste had all burnt up (≈60 min) then left to cool. The BB product was taken to study the physical and chemical properties.

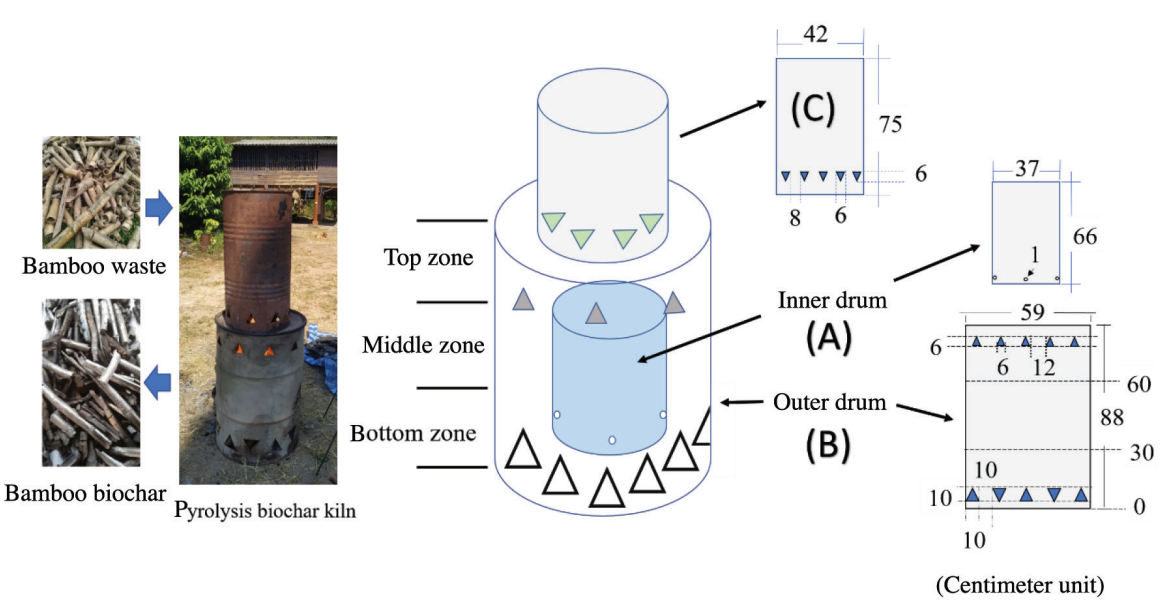

Fig. 2 Schematic diagram of bamboo biochar production

3. Characterization of BB

3.1 Proximate analysis

Proximate analysis is the composition of the moisture, ash, volatile matter and fix carbon and analyzed by modifying according to Aller, Bakshi, & Laird (2017). The moisture content of BB was determined based on weight loss after two hours at 110°C in hot air oven (Memmert, Germany) under N_2 purge. Volatile matter (VM) of BB (same sample) was carried out by heating a crucible containing the BB covered with ceramic lid placed in a stainless-steel box under nitrogen purge by muffle furnace to 950°C held 10 min at heating rate 2°C min^{-1} (THERMCONCEPT Ht40 Al, Germany). Ash content of BB was measured based on weight loss by heating the same sample to 730°C in an air atmosphere using the same muffle furnace and performed overnight (8-10 hours). After the ashing, the furnace was then switched off and let to cool before the sample was transferred to a desiccator. The moisture (% Moisture), volatile matter (% VM) and ash (% Ash) content were determined by equations 1, 2 and 3, respectively, as shown below.

$$\%\, Moisture = \left(\frac{W_I - W_D}{W_D}\right) * 100 \quad \text{(Eq. 1)}$$

$$\%\, VM = \left(\frac{W_D - W_V}{W_D}\right) * 100 \quad \text{(Eq. 2)}$$

$$\%\, Ash = \left(\frac{W_A}{W_D}\right) * 100 \quad \text{(Eq. 3)}$$

Where W_I, W_D, W_V and W_A were the weight (g) of BB of initial, oven drying at 110°C, after heat at 950°C and after combustion at 730°C overnight, respectively. Whereas, the fixed carbon is the carbon found in the biochar, which was left after moisture, volatiles and ash in the biochar were driven off. The percent fixed carbon (% FC) was calculated as equation 4 and is shown below.

$$\%\, FC = 100\% - (\%\, Moisture + \%\, VM + \%\, Ash) \quad \text{(Eq. 4)}$$

3.2 Ultimate analysis

The specific surface area and total pore volume of BB were analyzed by N_2 adsorption-desorption by Autosorb 1MP surface area analyzer (Quantachrome Instruments, USA). The BB sample was degassed under vacuum at 250°C performed overnight in order to eliminate the volatile matters before measuring. An elemental analyzer was used to determine CHN/O compositions (LECO CHNS model 932 elemental analyzer) through pyrolysis. The above techniques were analyzed by The Petroleum and Petrochemical College, Chulalongkorn University, Thailand. The oxygen content was calculated by difference. The pH value of BB was measured by a Starter 3100 bench, Ohaus pH meter. Two grams of BB was added into 50 cm^3 double distilled water, the mixture was shaken for 30 minutes at 150 rpm, then centrifuged and filtered. The filtrate was tested for the pH value.

3.3 Scanning electron microscopy (SEM) and energy-dispersive X-ray spectroscopy (EDS)

Scanning electron microscopy (SEM) and energy-dispersive X-ray spectroscopy (EDS) techniques allow for targeted analysis of sample surfaces that offer a direct way to observe the surface structure and mineral distribution of biochar. The BB surface morphology was investigated using a JEOL SEM analyzer JSM-6610 LV (JEOL Ltd., Tokyo, Japan) with an accelerating voltage of 20 kV. Meanwhile, the surface chemical elemental composition was determined by Energy Dispersion Spectrometry analysis (EDS, Oxford instrument X-Max 50 mm^2, England).

3.4 Infrared spectroscopy

Attenuated total reflection (ATR) - Fourier transform infrared spectroscopy (FTIR) was carried out to determine the functional groups of both the BB and feedstock. ATR-FTIR was performed using an IR Tracer-100 FTIR spectrophotometer (Shimadzu) with a diamond, zinc selenide (ZnSe) prism used in the ATR accessory. The number of scans was 40, with wide range at 4000 to 500 cm^{-1} at a resolution of 4 cm^{-1}. The background was collected before each measurement. The band positions were obtained using the LabSolutions IR control software.

3.5 Raman spectroscopy

Raman spectra of BB was carried out by using a Horiba LabRAM HR Evolution Raman Spectrometer. The spectra were acquired with a 50 LWD objective that were recorded from 650-2200 cm^{-1} with an excitation laser source of 532 nm, 100 mW, 3.2 to 5% power and using 20 accumulations. The instrument was controlled using LabSpec 6 software.

3.6 X-ray diffraction (XRD)

X-ray diffraction (XRD) analysis was used to investigate any crystallographic structure in the biochar. XRD pattern of the BB sample was identified using a Bruker D2 Phaser X-ray diffractometer (Bruker, Karlsruhe, Germany). It was operated in the 2θ range of 10-90^0 at 1^0 min^{-1} scan speed and step time 0.5^0 at room temperature.

3.7 Batch adsorption experiment

During August 2021, surface water was collected from Nakhon Nayok River, Sarika, Mueang Nakhon Nayok District, Nakhon Nayok Province, Thailand (14°14'46"N 101°16'37"E) as shown in Fig.1B. The physicochemical characteristics of raw water were as follows: pH: 7.54, DO 1.70-8.00, BOD 1.03-3.23 and N_{NH3} 0.01-1.43 mg L^{-1} (Regional Environmental Office 7, 2021). One hundred liters of surface water was collected with a black polyethylene container then brought to the laboratory. Pre-treatment included the water sample being filtered through 5 and 1 µm commercial polypropylene filter, 0.7 µm GF/C, 0.45 µm cellulose nitrate membrane (Whatman) and RO Membrane (ULTRATEK TW-1812-50 GPD) as shown in Fig. 3. Batch experiments were performed with NOM adsorption in an aqueous solution, 100 cm^3 of sample water and 1 g L^{-1} black powder adsorbent were placed in Erlenmeyer flasks (250 mL) shaken with 150 rpm at room temperature without pH adjustment. The kinetic was studied at intervals that varied between 1 minute and 48 hours. The collected samples, after batch test, were centrifuged at 3,000 rpm for 5 min before being filtered through 0.45 µm nylon membranes syringe filter to NOM measurement. In order to assess the NOM removal efficiency was analyzed for dissolved organic carbon (DOC) using Multi N/C 2100S-Direct injection TOC analyzer (Analytik Jena GmbH, Germany) and UV absorbance measurement at 254 nm (UV_{254}) wavelength in 1 cm quartz cells (Kearns et al., 2021), by a UV-1201 Shimadzu spectrophotometer. The efficiency removal of NOM and adsorption capacity were calculated by equations 5 and 6, respectively, as shown below.

$$\%\ NOM\ removal = \left(\frac{C_i - C_t}{C_i}\right) * 100 \quad \text{(Eq. 5)}$$

$$Adsorption\ capacity, Q_t(mg.g^{-1}) = \frac{(C_i - C_t)}{W} V \quad \text{(Eq. 6)}$$

Where C_i and C_t (mg L^{-1}) were DOC concentration at initial and at time t, respectively, V (L) was mixture volume and W (g) was BB weight. The NOM removal in UV_{254} absorption was calculated as: removal (%) = $[(A_0-A_t)/A_0] * 100$, where A_0 and A_t were the absorbance at 254 nm at time 0 and t, respectively.

Results and discussion

1. Temperature profile and production yield

Performance of the pyrolysis system has been defined in terms of reactor temperature profile, biochar yield, and characteristics of biochar obtained. The average temperature for different position on the outside of kiln are shown in Fig. 4. The results showed that the average of 3 zones outside temperature of the kiln obviously increased with time. The maximum temperatures of top zone, middle zone and bottom zone of the kiln, were 610.8, 605.4 and 597.3°C, respectively, as a result of heat transfer from combustion of the fuel bed at the top to bottom. It can be observed that the temperature of all zones increased from room temperature to maximum with an increase of time over 35 min and then decreased to 40 ± 1°C over 80 min. However, the inner container should not be opened, it was left for 2 hours, because biochar can ignite again. The process was observed to complete in about 4 hours. The percent average BB yield was 28.76 ± 2.21 from six pyrolysis batches. Proximate and ultimate analysis were carried out to evaluate the characteristics of the BB as shown in Table 1.

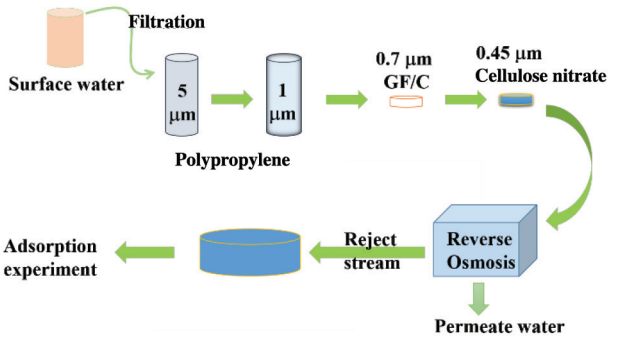

Fig. 3 Diagram prepare surface water sample to batch adsorption experiment

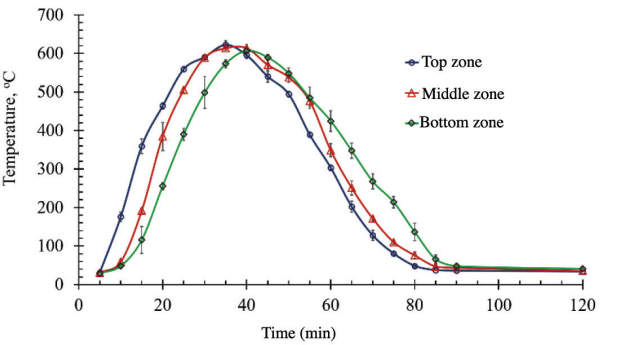

Fig. 4 The temperature profile of the outside kiln for different position

During pyrolysis process, cellulose, hemicellulose, lignin and fat of the biomass were thermally disintegrated over the temperature range between 150 and 400°C to

increase the carbon content by destroying oxygen, hydrogen and non-carbon species to gaseous products formed (Conte et al., 2021). After that, acid compounds, ketones, aldehydes, phenols, furans and guanidines were formed based on temperature between 400 and 700°C (Lewandowski et al., 2020). The weight loss of biomass from the thermal conversion to biochar was associated with decomposition of carbonates, sulfates and hydroxides, hydroxylation of some oxide compounds that affected to the surface area and pore of BB. In this study a surface analysis with specific surface area and pore volume of BB were 247.5 ± 7.1 m^2 g^{-1} and 0.16 ± 0.02 cm^3 g^{-1}, respectively. The drum kiln was developed from the traditional kiln and has been widespread to use for the biochar production in developing countries. Batch simple kiln technologies are usually the first choice for small farmers and start-up biochar producers before it can be improved into a large system that is widespread and has affordable price. In India and East Africa, forests are sustainably managed for biochar production using low-cost kiln as well as being more environmentally friendly and can reduce GHG emissions into the atmosphere by approximately 75%. Moreover, increased efficiency of biochar production was about 30%-40% better than the traditional biochar production method, which was about 10%-20% (Adam, 2009). Similarly, the kiln used in this research, had all wood gases released during carbonization and were controlled and burned as a fuel for the process to reduce emissions.

Table 1 Physical and chemical properties of the BB

Bamboo biochar properties	% Dry weight
Proximate analysisa	
Biochar yield	28.76 ± 2.22
Ash	6.58 ± 2.00
Moisture content	7.32 ± 1.00
Volatile	9.03 ± 1.77
Fix carbon	77.07 ± 1.92
pH	8.90 ± 0.51
Specific surface area (m^2/g)[b]	247.5 ± 7.1
Pore volume (cm^3/g)[b]	0.16 ± 0.02
Elemental analysis [b]	
C	65.17 ± 2.15
H	3.16 ± 0.05
N	0.77 ± 0.06
O*	30.94 ± 2.15
H/C	0.04
O/C	0.47

Remark: [a] n = 6, [b] n = 3, * By difference

2. Physical and chemical properties of the BB

Table 1 shows the elemental analysis of CHN/O chemical properties of the BB. The ratio of hydrogen to carbon (H/C) indicates aromaticity index to evaluate the degree of thermochemical change that produces fused aromatic ring structures in biochar while oxygen to carbon ratio (O/C) represents hydrophilicity index related to biochar stability. In the pyrolysis process, carbon, hydrogen and oxygen are eliminated in gases and volatile matters, as a result, the H/C and O/C ratios would decrease, corresponding to an increase in aromaticity and carbon content with an increase in pyrolysis temperature (Windeatt et al., 2014). The lower the H/C and O/C ratio used to indicate higher fused aromatic ring structure and higher stability in carbon fraction (Fernandes et al., 2020). The H/C and O/C ratio of BB in this study were 0.04 and 0.47, respectively, which indicated a high carbon content and higher stability in aromatic ring structures then would be preserved for at least 100 years in soil. This is consistent with the work done by Spokas (2010), which showed the O/C ratio in the range of 0.2–0.6. That means the dwell time of biochar in soil was about 100–1000 years.

The BB morphological characteristics obtained by scanning electron microscopy (SEM) and energy dispersive x-ray spectroscopy (EDS) is shown in Fig.5. Fig.5a shows obvious morphological of BB with a large surface area, tubular shapes, rough surface structures and sharp edges, approximate porous space of 12-15 µm spread on biochar surface. Moreover, at a magnification of 5,000X, a micropore was found within the mesopores in Fig.5b. In Fig.5c the BB cross-section shows mesopores structure spread on biochar surface and the surface pore morphology is similar to a honeycomb-like structure. The results of the SEM images of BB corresponded with the results of the surface analysis in which specific surface area and pore volume were influenced by the content of water and nutrients retained (Hernández-Mena et al., 2014). The C (76.32%) and O (16.77%) content as the major elements of the BB were indicated by EDS analysis and are shown in EDS analysis Fig. 5d. Furthermore, the other minerals, such as Mg, Si, P, S, Cl, K and Ca could be detected from six pyrolysis batches appearing in Table. 2. The results implied that C was the main skeleton with O in the BB, which may be influenced from oxygen-containing compounds (e.g. carboxylic -COOH, hydroxyl -OH, carbonate -CO_3^{2-}, phosphate -PO_4^{3-}or sulphate -SO_4^{2-}).

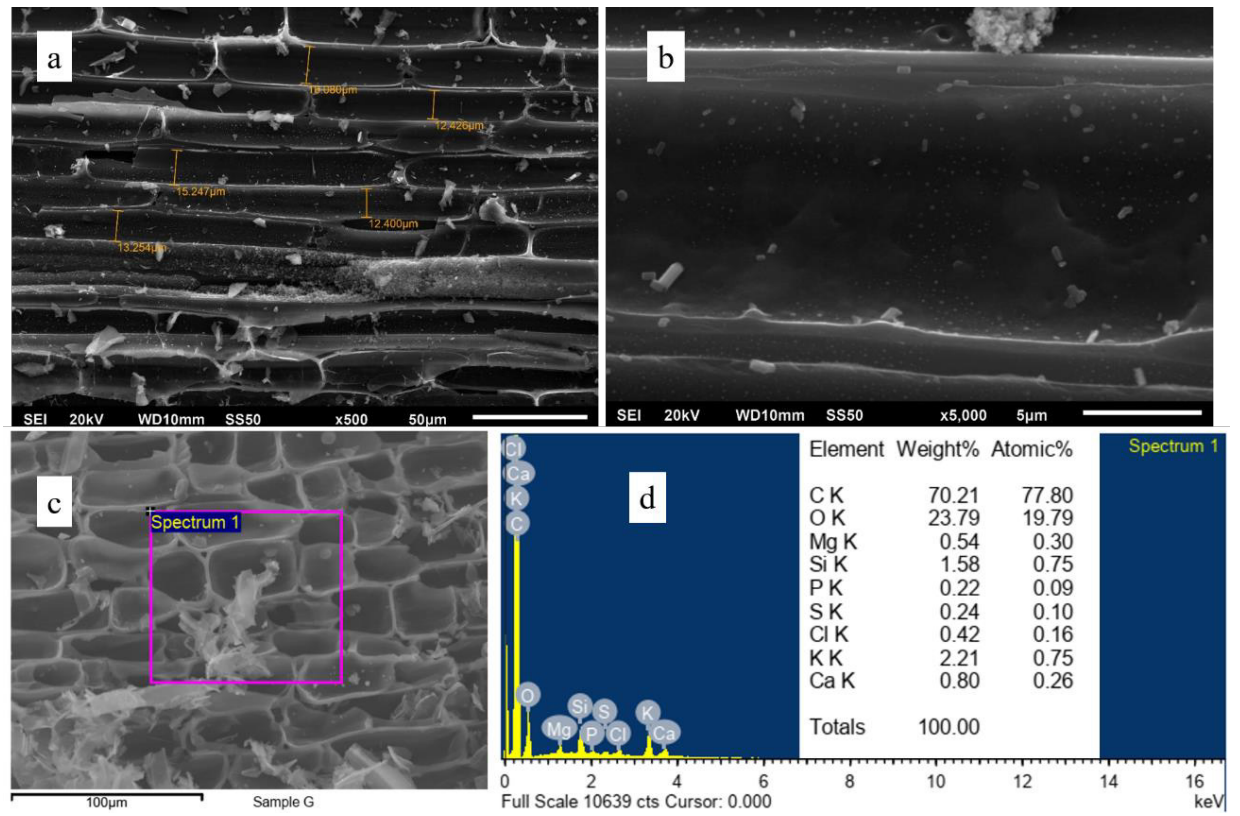

Fig. 5 SEM images of bamboo biochar: a and b were 500 and 5000 times magnification, respectively, c and d were EDS analysis

Table. 2 Element composition of BB by EDS analysis

Element	Average
C	76.32 ± 3.25
O	16.77 ± 3.02
Mg	0.43 ± 0.17
P	0.56 ± 0.16
Cl	0.61 ± 0.71
K	3.43 ± 3.28
Ca	0.64 ± 0.01
S	0.35 ± 0.14
Si	1.57 ± 1.60

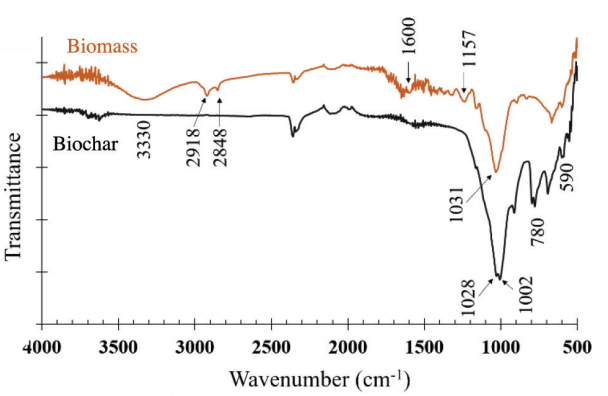

Fig. 6 ATR-FTIR spectra of raw bamboo biomass and its biochar

ATR-FTIR spectra of biomass and BB are shown in Fig.6. Lignocellulosic materials consisted of cellulose, hemicellulose and lignin indicating broad band between 3500 and 3000 cm^{-1} corresponding with O-H and N-H vibrations of phenol and amine and the C-H symmetric stretching at 2918 and 2848 cm^{-1} (Qin et al., 2020). The bamboo-derived biochar's with the band at the region of 3000-3500 cm^{-1} disappeared, hence signifying complete dehydration and de-oxygenation reactions at 600°C pyrolysis temperature. Recommending polar functional groups were reduced to hydrophobic material with very less functional groups were obtained (Ramola et al., 2014). The fingerprint region (1600 to 400 cm^{-1}) provided insight for disappearance of cellulose and hemicellulose in BB sample owing to the decomposition of the raw biomass. The spectra of biomass, a peak at 1600 cm^{-1} was assigned to the aromatic skeletal C=C and C=O vibration mode of hemicellulose and lignin (Nair et al.,

2020). The peak at 1031 cm^{-1} referred to the C-OH or C-O-C stretching vibrations of cellulose, hemicellulose and lignin (El-Sakhamed et al., 2018). Peaks for C–H bending bonds (out of plane) in the region of 900–675 cm^{-1}, which was characteristic of the aromatic substitution pattern, were clearly visible for biochars. The peak at 1000 cm^{-1} can be assigned to the C-O stretching vibration of alcohols and ester groups (Guizani et al., 2017). Silicates (Si-O) and phosphates (P-O) were displayed at the wideband around 1000 cm^{-1} that remained unchanged at temperatures below 700°C (Zhang et al., 2015; Cantrell et al., 2012). The 590 cm^{-1} peak obtained from iron oxide compounds or Fe–O–Si bond (Gotić & Musić, (2007) that forms in attendance of iron and silicate minerals at higher temperatures.

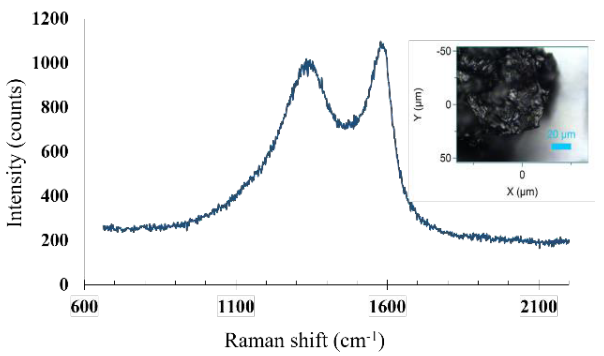

Fig. 7 Raman spectrum of bamboo biochar

Raman Spectroscopy is an outstanding method for characterizing carbon materials. Raman spectrum of the BB appeared at maximum intensity at 1348 cm^{-1} and 1588 cm^{-1}, which is in accordance with the D and G bands of the graphitic-like structures, respectively, shown in Fig. 7. Both D and G peaks are the result of vibrations of sp^2-bonded carbon atoms. The D band is due to out of plane vibrations of sp^2-bonded carbon attributed to the presence of structural defects whereas the G band is formed by sp^2 bonded crystallite carbon vibration both in rings and chains of the graphite crystalline plane. (Ferrari & Robertson, 2000). The intensity ratio between the D and G bands can be used to estimate the degree of crystallinity of carbon-containing materials. The high D/G intensity ratio of BB was 0.868 (in Fig.7) indicating the pyrolysis temperature was greater than 600°C (Gonzalez-Canche et al., 2021).

X-ray diffraction analysis is performed to assess a degree of crystalline or amorphous structure in a sample. The XRD diffractogram of BB contained mainly the

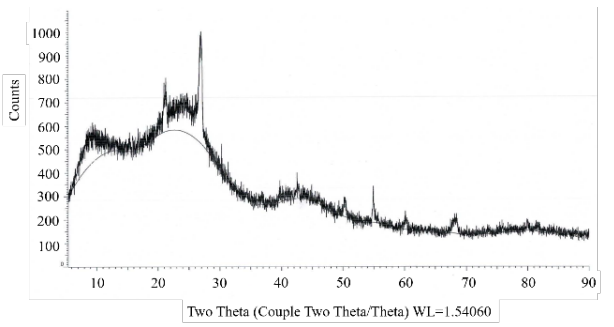

Fig. 8 XRD characterization of bamboo biochar

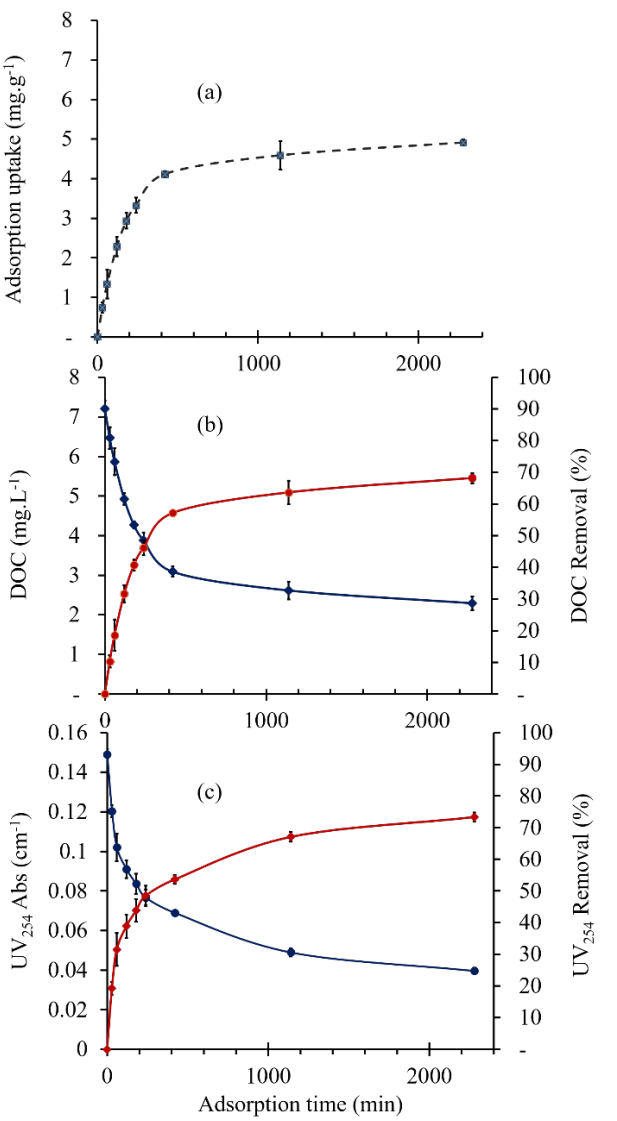

Fig. 9 NOM removal, (a) adsorption efficiency, (b) DOC reducing, (c) UV254 absorbance reducing

amorphous compounds were indicated in Fig. 8. The two theta (2θ) wide range 20˚-30˚ refers to the stacking structure of the aromatic layer (Liu et al., 2012). Sharp crystalline non-labeled peaks in BB diffractogram probably indicated the miscellaneous inorganic components, such as these peaks are consistent with the higher content of SiO_2 (quartz, 2θ = 20.86˚, 26.62˚) and $CaCO_3$ (calcite, 2θ = 50.58˚), corresponding with Sackey et al., (2021) research.

3. Removal of NOM

Application of BB for NOM removal in Nakhon Nayok River, Thailand was investigated. The amount of NOM was represented in DOC concentration and UV absorbance at 254 nm measurement. The initial content of DOC and UV_{254} were 7.21 ± 0.20 mg L^{-1} and 0.149 ± 0.002 cm^{-1}, respectively. The high values of DOC and UV_{254} were due to the samples being collected in August, which was the rainy season and soils rich in organic matter was transported into the water by run-off (Singh & Choden, 2014). The effect of adsorption time on the removal of NOM is shown in Fig. 9. The adsorption capacity of the DOC on BB increased with the extension of contact time. In the first 6 hours the adsorption capacity grew rapidly after that the adsorption tended to equilibrium gradually (Fig.9(a)) and the adsorption efficiency of equilibrium was 4.75 mg g^{-1}. Fig. 9 (b) and (c) shows that the adsorption rate of DOC and UV_{254} on BB were initially fast and then gradually reduced until equilibrium was reached. More than 50% of DOC and UV_{254} were removed within contact time 6 hours of 1 g L^{-1} BB in the first stage. A slower phase occurred thereafter with equilibrium being achieved within 48 hours, corresponding to about 70% removal.

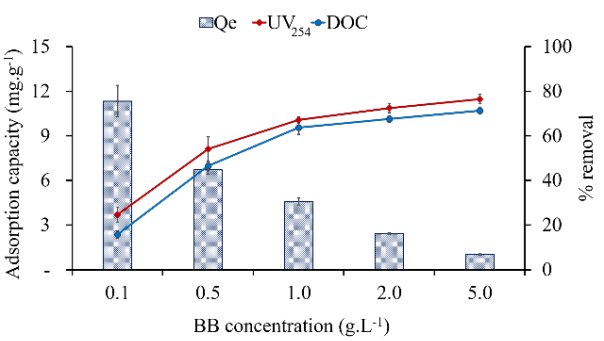

Fig. 10 Effect of adsorbent concentration on DOC adsorption

The effect of BB dose was evaluated by varying adsorbent dosage in the range from 0.01 to 0.5 g of adsorbent in 100 cm^3 water sample. It is clear from Fig. 10 that the removal percentage of the DOC and UV_{254} had a direct proportional to adsorbent dosage from 15.71 ± 1.44 to 71.33 ± 1.46% and 24.60 ± 3.31 to 76.51 ± 2.01, respectively. Whereas the adsorption efficiency of DOC on BB at equilibrium (Q_e) decreased from 11.33 ± 1.04 to 1.03 ± 0.02 mg g^{-1} with an increase in adsorbent dose 0.1 to 5.0 g L^{-1} shown in Fig.10. The increased of the adsorbent dose effected the number of active sites and thus removal percentage improved. However, the adsorbent high content may be due to aggregation of adsorbent, which would lead to a reduction in the adsorbent capacity through decreasing the total surface area causing the site to be less active thus resulting in the lower number of DOC molecules per active site.

The adsorption kinetics of BB was educated based on the above adsorption equilibrium results of DOC. The adsorption kinetic model of DOM onto BB was assessed by using pseudo-first-order and pseudo-second-order kinetic models as shown below by equations 7 and 8, respectively.

$$log(Q_e - Q_t) = logQ_e - \frac{k_1}{2.303}t \quad \text{(Eq. 7)}$$

$$\frac{t}{Q_t} = \frac{1}{k_2 Q_e^2} + \frac{1}{Q_e}t \quad \text{(Eq. 8)}$$

Where Q_e and Q_t are the biochar adsorption uptake (mg g^{-1}) at equilibrium time and any time t (min), respectively, the adsorption rate constants k_1 (min^{-1}) and k_2 (g mg^{-1} min^{-1}) are primary and secondary constants, respectively. A plotting of log (Q_e-Q_t) versus time in Eq.7 and of t/Q_t versus time in Eq.8 both yields a straight line as shown in Fig.11. The rate constant (k_1) and absorption capacity (Q_e) of the pseudo-first-order reaction can be determined from the slope of the straight line and intercept of the plot in Fig. 11 (blue line), respectively. Similarly, the rate constant (k_2) and equilibrium absorption capacity (Q_e) of the pseudo-second-order reaction were determined from the intercept and slope of a linear relationship in Fig. 11 (red line). According to the equation 7 and 8 given above, the kinetic parameters were calculated and appeared in Table 3. It was clear from the correlation coefficient, R^2 values given in Table 3 that pseudo-second-order kinetic model was greater than pseudo-first-order kinetic model,

which best describes the adsorption of DOC on BB. This suggests that the interaction of NOM on BB were explored in terms of multicomponent adsorption of its different fractions as chemical nature, functional groups present on the surface, pore filling, π–π interactions, polar/electrostatic interactions, hydrophobic effect and hydrogen bonding (Yazdani et al., 2019; Ahmad et al., 2014).

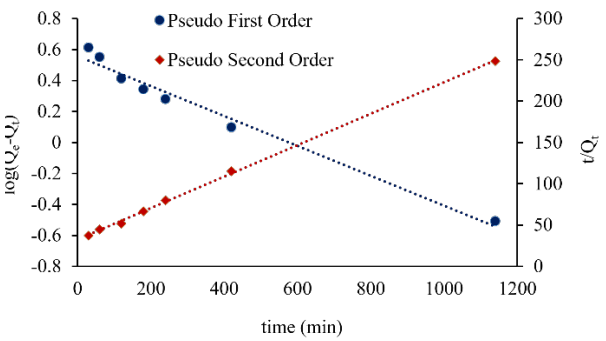

Fig. 11 Adsorption kinetic model of DOC removal

Table 3 Adsorption kinetic parameters of DOC on BB

Parameter	Pseudo-first-order	Pseudo-second-order
Adsorption rate constant, k	0.0023 (min^{-1})	0.0011 (g mg^{-1} min^{-1})
Q_e (mg g^{-1})	3.607	5.254
R^2	0.9783	0.9992

Conclusion

The production temperature (500–600°C) and heating time of about 1 hour for biochar produced in this research kiln were closely related to slow pyrolysis. The process was observed to complete in about 4 hours with the% BB yield of 28.76 ± 2.21 of dry weight. The BB high quality were characterized by BET, SEM-EDS, ATR-FTIR, Raman spectroscopy, XRD, proximate analysis and elemental composition revealed macro-meso-and micro-pore structure, high surface area was 247.5 ± 7.1 m^2 g^{-1} and 0.16 ± 0.02 cm^3 g^{-1} of pore volume, 77.07 ± 1.92% fix carbon, amorphous structure mixed of sp^2 and sp^3 carbon bonds and surface functionality. The absorbent product was applied to remove NOM in Nakhon Nayok River, Thailand, and could reduce 50% at 6 hours contact time with 1 g L^{-1} of BB. The absorption efficiency at equilibrium and maxima removal were 4.75 mg g^{-1} and about 70%, respectively following pseudo-second-order kinetic model. Suggestions for further research should study if BB may be used to eliminate heavy metals in local community groundwater. The results in this study cannot be generalized across kiln design and starting biomass feedstock, nevertheless it represents that our simple kiln can produce good quality biochar from bamboo waste. In addition, the biochar kiln is also small and easy to create and use as well as producing no smoke, inexpensive, does not take a lot of time to produce and has an eco-friendly processing.

Acknowledgment

This research was supported by Suan Dusit University, Thailand

References

Adam, J.C. (2009). Improved and more environmentally friendly charcoal production system using a low-cost retort-kiln (Eco-charcoal). *Renew Energ, 34,* 923–925

Ahmad, M., Rajapaksha, A.U., Lim, J.E., Zhang, M., Bolan, N., Mohan, D., ... Ok, Y.S. (2014). Biochar as a sorbent for contaminant management in soil and water: A review. *Chemosphere, 99,* 19-33.

Al-Ghussain, L. (2019). Global warming: review on driving forces and mitigation. *Environmental Progress & Sustainable Energy, 38*(1), 13-21.

Aller, D., Bakshi, S., & Laird, D.A. (2017). Modified method for proximate analysis of biochars. *Journal of Analytical and Applied Pyrolysis, 124,* 335-342.

Arunrat, N., Pumijumnong, N., & Sereenonchai, S. (2018). Air-pollutant emissions from agricultural burning in Mae Chaem Basin, Chiang Mai province, Thailand. *Atmosphere, 9*(4), 145.

Cantrell, K.B., Hunt, P.G., Uchimiya, M., Novak, J.M., & Ro, K.S. (2012). Impact of pyrolysis temperature and manure source on physicochemical characteristics of biochar. *Bioresource Technology, 107,* 419–428.

Conte, P., Bertani, R., Sgarbossa, P., Bambina, P., Schmidt, H.P., Raga, R., ... Lo Meo, P. (2021). Recent developments in understanding biochar's physical–chemistry. *Agronomy, 11*(4), 615.

Dokmaingam, P., Kongkratoke, S., Anuwatnonthakate, A., & Yongprapat, S. (2020). The improvement of hydroponics growth media by using the corncob biochar. *Journal of Food Health and Bioenvironmental Science, 13*(3), 26-31

El-Hassanin, A.S., Samak, M.R., Radwan, S.R., & El-Chaghaby, G.A. (2020). Preparation and characterization of biochar from rice straw and its application in soil remediation. *Environment and Natural Resources Journal, 18*(3), 283-289.

El-Sakhawy, M., Kamel, S., Salama, A., & Tohamy, H.A.S. (2018). Preparation and infrared study of cellulose based amphiphilic materials. *Journal of Cellulose Chemistry Technology, 52*(3-4), 193-200.

Fernandes, B.C.C., Mendes, K.F., Dias Júnior, A.F., da Silva Caldeira, V.P., da Silva Teófilo, T.M., Severo Silva, T., ... Valadão Silva, D. (2020). Impact of pyrolysis temperature on the properties of eucalyptus wood-derived biochar. *Materials, 13*(24), 5841.

Ferrari, A.C., & Robertson, J. (2000). Interpretation of Raman spectra of disordered and amorphous carbon. *Physical Review B, 61*(20), 14095.

Ghernaout, D., Moulay, S., Ait Messaoudene, N., Aichouni, M., Naceur, M.W., & Boucherit, A. (2014). Coagulation and chlorination of NOM and algae in water treatment: A review. *International Journal of Environmental Monitoring and Analysis, 2*(6-1), 23-34.

Gonzalez-Canche, N.G., Carrillo, J.G., Escobar-Morales, B., Salgado-Tránsito, I., Pacheco, N., Pech-Cohuo, S.C., & Peña-Cruz, M.I. (2021). Physicochemical and optical characterization of *Citrus aurantium* derived biochar for solar absorber applications. *Materials, 14*(16), 4756.

Gotić, M., & Musić, S. (2007). Mössbauer, FT-IR and FE SEM investigation of iron oxides precipitated from $FeSO_4$ solutions. *Journal of Molecular Structure, 834,* 445-453.

Guillossou, R., Le Roux, J., Mailler, R., Pereira-Derome, C.S., Varrault, G., Bressy, A., ... Gasperi, J. (2020). Influence of dissolved organic matter on the removal of 12 organic micropollutants from wastewater effluent by powdered activated carbon adsorption. *Water Research, 172,* 115487.

Guizani, C., Jeguirim, M., Valin, S., Limousy, L., & Salvador, S. (2017). Biomass chars: The effects of pyrolysis conditions on their morphology, structure, chemical properties and reactivity. *Energies. 10*(6), 796.

He, J., Li, Y., Cai, X., Chen, K., Zheng, H., Wang, C., ... Liu, J. (2017). Study on the removal of organic micropollutants from aqueous and ethanol solutions by HAP membranes with tunable hydrophilicity and hydrophobicity. *Chemosphere, 174,* 380-389.

Hernández-Mena, L.E., Pécoraa, A.A., & Beraldob, A.L. (2014). Slow pyrolysis of bamboo biomass: analysis of biochar properties. *Chem. Eng., 37,* 115-120.

Kätterer, T., Roobroeck, D., Andrén, O., Kimutai, G., Karltun, E., Kirchmann, H., ... de Nowina, K.R. (2019). Biochar addition persistently increased soil fertility and yields in maize-soybean rotations over 10 years in sub-humid regions of Kenya. *Field Crops Research, 235,* 18-26.

Kearns, J., Dickenson, E., Aung, M.T., Joseph, S.M., Summers, S.R., & Knappe, D. (2021). Biochar water treatment for control of organic micropollutants with UVA surrogate monitoring. *Environmental Engineering Science, 38*(5), 298-309.

Land Development Department, (2020). *The proportion of area under bamboo cultivation in various regions of the country.* Retrieved October 30, 2021, from http://www1.ldd.go.th/WEB_OLP/Lu_62/Lu62_C/NYK2562.htm

Lewandowski, W.M., Ryms, M., & Kosakowski, W. (2020). Thermal biomass conversion: A review. *Processes, 8*(5), 516.

Liu, Y., Zhao, X., Li, J., Ma, D., & Han, R. (2012). Characterization of bio-char from pyrolysis of wheat straw and its evaluation on methylene blue adsorption. *Desalination Water Treat., 46*(1-3), 115-123

Lohan, S.K., Jat, H.S., Yadav, A.K., Sidhu, H.S., Jat, M.L., Choudhary, M., ... Sharma, P.C. (2018). Burning issues of paddy residue management in north-west states of India. *Renewable and Sustainable Energy Reviews, 81,* 693-706.

Nair, R.R., Mondal, M.M., & Weichgrebe, D. (2020). Biochar from co-pyrolysis of urban organic wastes-investigation of carbon sink potential using ATR-FTIR and TGA. *Biomass Conversion and Biorefinery,* 1-15.

Nguyen, T.T., Chen, H.H., To, T.H., Chang, Y.C., Tsai, C.K., Chen, K.F., & Tsai, Y.P. (2021). Development of biochars derived from water bamboo (*Zizania latifolia*) shoot husks using pyrolysis and ultrasound-assisted pyrolysis for the treatment of reactive black 5 (RB5) in Wastewater. *Water, 13*(12), 1615.

O'Toole, A., Knoth de Zarruk, K., Steffens, M., & Rasse, D.P. (2013). Characterization, stability, and plant effects of kiln-produced wheat straw biochar. *Journal of Environmental Quality, 42*(2), 429-436.

Qin, L., Wu, Y., Hou, Z., & Jiang, E. (2020). Influence of biomass components, temperature and pressure on the pyrolysis behavior and biochar properties of pine nut shells. *Bioresource Technology, 313,* 123682.

Ragional Environmental Office 7. (2021). *Report: Surface water quality,* Retrieved October 30, 2021, from http://www.reo07.mnre.go.th/th/information/list/2051

Ramola, S., Mishra, T., Rana, G., & Srivastava, R.K. (2014). Characterization and pollutant removal efficiency of biochar derived from baggase, bamboo and tyre. *Environmental Monitoring and Assessment, 186*(12), 9023-9039.

Sackey, E.A., Song, Y., Yu, Y., & Zhuang, H. (2021). Biochars derived from bamboo and rice straw for sorption of basic red dyes. *Plos One, 16*(7), e0254637.

Shaheen, S.M., Niazi, N.K., Hassan, N.E., Bibi, I., Wang, H., Tsang, D.C., ... Rinklebe, J. (2019). Wood-based biochar for the removal of potentially toxic elements in water and wastewater: A critical review. *International Materials Reviews, 64*(4), 216-247.

Singh, H., & Choden, S. (2014). Comparison of adsorption behaviour and kinetic modeling of bio-waste materials using basic dye as adsorbate. *Indian J. Chem. Technol., 21,* 359–367.

Song, X., Li, Y., Yue, X., Hussain, Q., Zhang, J., Liu, Q., ... Cui, D. (2019). Effect of cotton straw-derived materials on native soil organic carbon. *Science of the Total Environment, 663,* 38-44.

Spokas, K.A. (2010). Review of the stability of biochar in soils: Predictability of O: C molar ratios. *Carbon Management, 1*(2), 289-303.

Srivatsav, P., Bhargav, B.S., Shanmugasundaram, V., Arun, J., Gopinath, K.P., & Bhatnagar, A. (2020). Biochar as an eco-friendly and economical adsorbent for the removal of colorants (dyes) from aqueous environment: A review. *Water, 12*(12), 3561.

Wang, X., Guo, Z., Hu, Z., & Zhang, J. (2020). Recent advances in biochar application for water and wastewater treatment: A review. *PeerJ, 8,* e9164.

Windeatt, J.H., Ross, A.B., Williams, P.T., Forster, P.M., Nahil, M.A., & Singh, S. (2014). Characteristics of biochars from crop residues: potential for carbon sequestration and soil amendment. *Journal of Environmental Management, 146,* 189-197.

Yazdani, M.R., Duimovich, N., Tiraferri, A., Laurell, P., Borghei, M., Zimmerman, J.B., & Vahala, R. (2019). Tailored mesoporous biochar sorbents from pinecone biomass for the adsorption of natural organic matter from lake water. *Journal of Molecular Liquids, 291,* 111248.

Yehia, H.M. A.S., & Said, S.M. (2021). Drinking water treatment: pH adjustment using natural physical field. *Journal of Biosciences and Medicines, 9*(6), 55-66.

Zhang, X., Gao, B., Zheng, Y., Hu, X., Creamer, A.E., Annable, M.D., & Li, Y. (2017). Biochar for volatile organic compound (VOC) removal: Sorption performance and governing mechanisms. *Bioresource Technology, 245,* 606-614.

Zhang, J., Lü, F., Zhang, H., Shao, L., Chen, D., & He, P. (2015). Multiscale visualization of the structural and characteristic changes of sewage sludge biochar oriented towards potential agronomic and environmental implication. *Scientific Reports, 5*(1), 1-8.